3D MODELING OF HIGH RELIEF SCULPTURE USING IMAGE BASED INTEGRATED MEASUREMENT SYSTEM

T. Ohdake [a, *], H. Chikatsu [a]

[a] Tokyo Denki Univ., Dept. of Civil and Environmental Engineering,
350-0394 Hatoyama, Saitama, Japan - (ohdake, chikatsu)@g.dendai.ac.jp

Commission V, WG V/4

KEY WORDS: Photogrammetry, Calibration, Camera, Laser, Modelling, Integration, System

ABSTRACT:

A convenient 3D measurement using amateur digital camera is enormously expected in various fields with appearance of the low cost and high-resolution amateur digital cameras. In these circumstances, there are many software for digital photogrammetry on the market in Japan. However, there are still problems for efficient digital photogrammetry. These problems include distance measurement for absolute orientation and interior orientation which should be performed beforehand, and these restrictions should be removed for ideal convenient photogrammetry using amateur digital cameras.
With this objective, Image Based Integrated Measurement System called as IBIM system was developed by the authors. The most remarkable point of the system is its ability to calculate both of exterior and interior orientation parameters without scale distance nor Ground Control Points which have exact 3D coordinates in object field. After the IBIM system and performance evaluation are briefly discussed, its application to 3D modelling of high relief sculpture is investigated in this paper.

1. INTRODUCTION

There are many digital cameras which have more than 5 mega pixels on the market in Japan. In these circumstances, a convenient 3D measurement using amateur digital camera is enormously expected from various fields, and there are many software for digital photogrammetry on the market.
In these circumstances, performance evaluations for the amateur digital cameras were investigated by the authors from the view point of digital Photogrammetry (Kunii and Chikatsu, 2001). The authors also have been concentrating on developing a convenient 3D measurement method using amateur digital camera, and software "3DiVision" was designed to perform convenient 3D measurement (Chikatsu and Kunii, 2002). However, there were some issues for practical 3D measurement using amateur digital camera. These problems were distance measurement for giving scale in absolute orientation and interior orientation which should be performed beforehand, and these restrictions should be removed for ideal convenient photogrammetry using amateur digital camera.
In order to remove these restrictive conditions and to promote a convenient digital photogrammetry using amateur digital camera, Image Based Integrated Measurement System which is called as IBIM system was developed, and calibration method was investigated by the authors (Odake and Chikatsu, 2004). The most remarkable point of the system is its ability to calculate both exterior and interior orientation parameters simultaneously without scale distance nor GCP.
After the IBIM system and performance evaluation are briefly discussed, its application to 3D modelling of historical wooden sculpture is investigated in this paper from the view point of "cultural heritage online project".

2. IBIM SYSTEM

The IBIM system consists of amateur digital camera (OLYMPUS C-770 Ultra Zoom, 4.0 mega pixels) and laser distance meter (Leica DISTO Lite 4, accuracy is ±3mm to 100m), and it is able to rotate in vertically and horizontally so that precise distance from centre of the camera to the feature points on object field can be measured, and images are record on SD memory card of the camera. Furthermore, camera and laser axis can be precisely adjusted using 4 adjusting screw on the eaves. Figure 1 shows an appearance of the IBIM system, and Figure 2 shows configuration of the system.

Figure 1. Appearance of the IBIM system

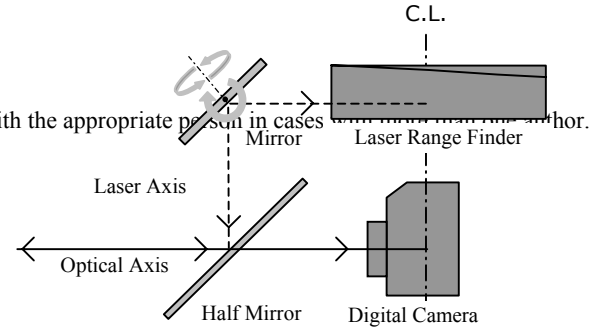

* Corresponding author. This is useful to know for communication with the appropriate person in cases with more than one author.

Figure 2. Configuration of the IBIM system

3. CAMERA CALIBRATION

3.1 Self-calibration

In order to perform camera calibration, at least 6 distances from center of the camera to the points which show feature on object have to be measured by the laser distance meter. These feature points are defined as temporal GCP in this paper. Then, 37 unknown parameters such as exterior orientation parameters for both camera {(X_{OL}, Y_{OL}, Z_{OL}, ω_L, φ_L, κ_L), (X_{OR}, Y_{OR}, Z_{OR}, ω_R, φ_R, κ_R)}, interior orientation parameters {f (focal length), x_0, y_0 (principal points), a_1, a_2 (scale factor), k_1, k_2 (lens distortion)} and 3D coordinates for 6 temporal GCPs should be calculated. Generally, number of unknown parameters become 19+3n (n: number of temporal GCPs), and these unknown parameters are calculated by collinearity condition and distances simultaneously under the geometric condition that one point is origin point and X direction is given. For example, 3D coordinate is given as P_1(0,0,0) for origin point and X direction is given as P_2(X_2,0,0) in the Figure 3. Then, 19+3n-5 becomes unknowns against 2n(distances)+ $2\times 2n$ (collinearity) conditions, and these unknowns can be calculated as the values which make following function H minimum under the least square method.

$$H = \sum_{i=1}^{M}\sum_{j=1}^{N}\left(p_1\left(\Delta x_{ij}{}^2 + \Delta y_{ij}{}^2\right) + p_2\left(\Delta D_{ij}{}^2\right)\right) \Rightarrow \min \tag{1}$$

where, Δx, Δy: residuals for image coordinate, ΔD: residuals for distance, M: number of temporal GCP, N: number of image, p_1,p_2: weight

Here, collinearity condition is shown as equation (2), and distance condition is shown as equation (3).

$$\begin{cases} x = f\dfrac{m_{11}(X-X_0)+m_{12}(Y-Y_0)+m_{13}(Z-Z_0)}{m_{31}(X-X_0)+m_{32}(Y-Y_0)+m_{33}(Z-Z_0)} \\ y = f\dfrac{m_{21}(X-X_0)+m_{22}(Y-Y_0)+m_{23}(Z-Z_0)}{m_{31}(X-X_0)+m_{32}(Y-Y_0)+m_{33}(Z-Z_0)} \end{cases} \tag{2}$$

where, x, y: image coordinate, X, Y, Z: Ground coordinate、m_{11}-m_{33}: Rotation matrix

$$D_i = \sqrt{(X_i-X_0)^2+(Y_i-Y_0)^2+(Z_i-Z_0)^2} \tag{3}$$

Furthermore, following radial polynomial 5th degree was adapted to correct lens distortion in this paper (Fryer J. G. and Brown D.C, 1986),

$$\begin{cases} dx = k_1\cdot r^2\cdot x' + k_2\cdot r^4\cdot x' \\ dy = k_1\cdot r^2\cdot y' + k_2\cdot r^4\cdot y' \end{cases} \tag{4}$$

where, $r = \sqrt{x'^2 + y'^2}$, x', y': image coordinate not-corrected, dx, dy: value of correction

and a_1 and a_2 are coefficient in following affine transformation which is obtained from relationship between pixel and image coordinate.

$$\begin{cases} u = u_0 + a_1\cdot x + a_2\cdot y \\ v = v_0 + a_3\cdot x + a_4\cdot y \end{cases} \tag{5}$$

where, (u,v):pixel coordinate, (x,y): image coordinate, (u_0,v_0), (x_0,y_0): coordinate of principal point

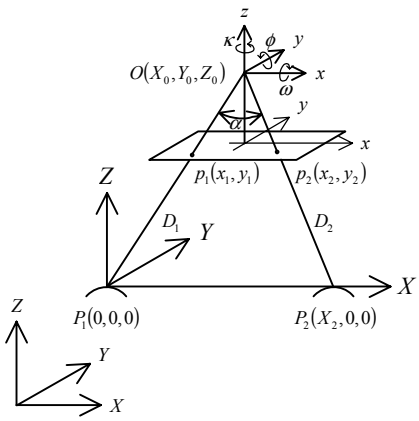

Figure 3. Geometry in the IBIM

However, initial values for camera position are required as same as orientation parameters in camera calibration, and these are obtained by following procedures.

Let make D_1 and D_2 in Figure 3 shows measured distances, angle α is computed with respect to focal length (f) and image coordinates by equation (6),

$$\cos\alpha = \frac{x_{p1}\cdot x_{p2} + y_{p1}\cdot y_{p2} + f^2}{\overline{Op_1}\cdot\overline{Op_2}} \tag{6}$$

where, $\overline{Op_1} = \sqrt{\left(x_{p1}{}^2 + y_{p1}{}^2 + f^2\right)}$, $\overline{Op_2} = \sqrt{\left(x_{p2}{}^2 + y_{p2}{}^2 + f^2\right)}$

and initial value X_2 for the point P_2 according to the origin point P_1 (0, 0, 0) is computed as L from following equation (7).

$$L = \overline{P_1P_2} = \sqrt{D_1{}^2 + D_2{}^2 - 2\cdot D_1\cdot D_2\cdot\cos\angle\alpha} \tag{7}$$

Therefore, right and left camera position O (X_0, Y_0, Z_0) can be estimated respectively as follows under assumption that vertical photo was taken over flat terrain.

$$X_0 = \left(D_1^2 - D_2^2 + L^2\right)/2L$$
$$Y_0 = D_1 \cdot \sin\left(-\left(\left(y_{p2} - y_{p1}\right)/f\right)\right) \quad (8)$$
$$Z_0 = D_1^2 - X_0^2 - Y_0^2$$

However, initial value for camera position which are computed from above equation (8) are value that are obtained under vertical photo. Then, initial value for exterior orientation parameters (camera position and attitude except κ) are recomputed using collinearity condition for P_1 and P_2, and distance for D_1 and D_2. κ is estimated in this step as 0°since the IBIM is set up on tripod with levelling function.

After above procedure, initial values for temporal GCPs for P_3 to P_n are computed using initial exterior orientation parameters, then self-calibration are performed by equation (1) using initial values and equal weight (P_1=P_2=1).

3.2 Measurement using the IBIM

Figure 4 shows measuring concept by the IBIM. After imaging at left position (A), distances for the *n* (6 in Figure 4) temporal GCPs are measured by rotating the IBIM, and repeat same procedures at right position (B).

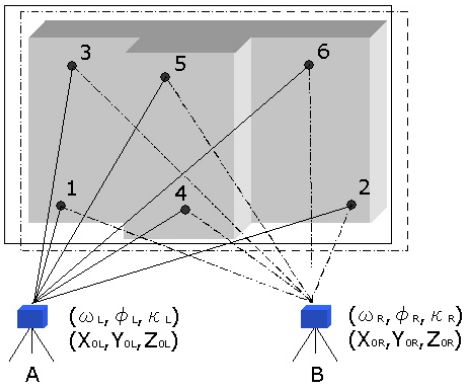

Figure 4. Concept of measurement by the IBIM

4. PERFORMANCE EVALUATION OF IBIM

In order to evaluate the IBIM system, test target (H:640mm, W:480mm, D:50mm) was used. Figure 5 shows test target. Each black circle point was manufactured with 0.05mm accuracy and 42 points (intersection of grid) were used as check points, and these image coordinates were obtained as area gravity by image processing procedures.

A point means origin point such as P_1, and B point shows X axis such as P_2 in Figure 3. 6 white circled points were temporal GCPs, and image coordinate for these points were measured by manually, since the laser's spot size is greater than the object-space resolution of the digital camera.

Stereo image was taken about 1.0m altitude respectively and 0.4 m base line under focal length was fixed, and distances were measured.

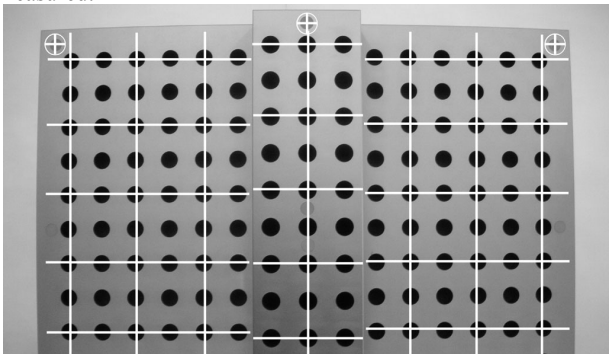

Figure 5. Test Target

Table 1 and 2 shows calibration results, and table 3 shows root mean square error for 42 check points. σ_{XY} means horizontal error and σ_Z means vertical error. Theoretical error which compute from equation (9) using altitude, base line, focal length and pointing accuracy is widely used in photogrammetry to estimate accuracy (Fraser, 1996).

$$\left.\begin{aligned}\sigma_{xy} &= \left(\frac{H}{f}\right)\sigma_p \\ \sigma_z &= \left(\frac{H}{f}\right)\left(\frac{H}{B}\right)\sigma_p\end{aligned}\right\} \quad (9)$$

where, *H*: altitude, *f*: focal length, *B*: base line, σ_p: pointing accuracy and it was estimated as 0.003mm in this paper.

Table 1. Exterior orientation parameters

	Left	Right
X_0	118.539 mm	525.384 mm
Y_0	216.482 mm	216.063 mm
Z_0	1019.188mm	1019.741 mm
ω	0° 27′ 12″	0° 24′ 34″
ϕ	5° 10′ 17″	-6° 30′ 12″
κ	-0° 01′ 11″	-0° 09′ 46″

Table 2. Interior orientation parameters

x_0	1144.731 pixels	a_1	397.2217
y_0	863.735 pixels	a_2	0.0087
f	6.810 mm	k_1	3.8874E-008
		k_2	-9.8098E-015

Table 3. Accuracy

	σ_{XY}	σ_Z
IBIM	± 0.587 mm	± 0.921 mm
Theoretical error	± 0.407 mm	± 1.019 mm

From Table 3, it can be said that both accuracy for XY and Z coordinate shows good results, and it is concluded that the calibration method was effective method for the IBEM.

5. APPLICATION TO 3D MODELING

5.1 Kangiin Shoutendo

Kangiin Shoutendo is located at Menuma, Saitama, was rebuilt at 1760 after spending 25 years. Shoutendo is one of famous temples in Japan from the viewpoint of elaborate and splendid sculptures which decorate back and side of the temple (Figure

6), and the temple was designated as important national cultural property at 1984.
These sculptures (each sculpture about 2m× 2m) were made of keyaki as a panel board, and theses are high relief sculptures. Thus, the high relief sculptures form extremely complex structure such as shown in Figure 6.
In order to investigate an adaptability of the IBIM system to recording and modeling of complex structures in architecture and archaeology, part of one sculpture (Figure 7) was measured by the IBIM.

Figure 6. Sculptures as a panel board

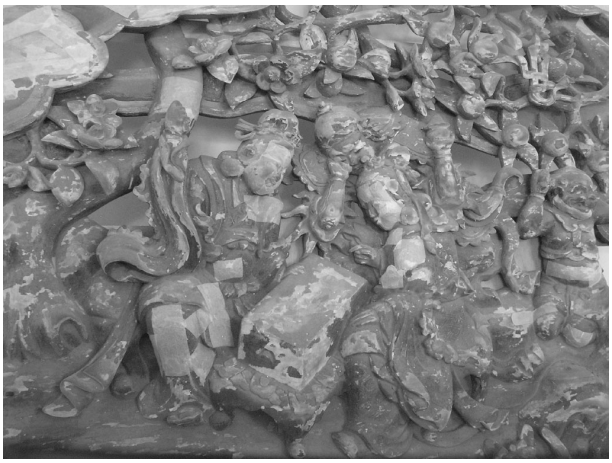

Figure 7. High relief sculpture

5.2 Outline of measurement by IBIM

Due to high relief sculpture was formed with curved lines and curved surfaces, dots laser projector was used to generate temporal GCPs efficiently.
Image was taken about 1.2m altitude with fixed focal length, and 6 distances for the temporal GCPs were measured at left position. Same procedure was repeated at right position with 0.9m base line.
In order to complement occlusion parts, additional stereo pair were taken by digital camera (CANON EOS 20D, 8.2 Mega pixels). Figure 8 shows camera position.

Figure 8. Camera position for stereo pairs

After above procedures, self-calibration was performed using equation (1) which were already mentioned in chapter 3.1.

5.3 Image Enhancement

Generally, TIN models used to generate using feature points for 3D modelling. It was predicted, however, 3D model which was generated by TIN doesn't show reality for curved surface objects.
Therefore, matching algorithm for all pixels were investigated in this paper, and in order to perform matching, image enhancement was performed as pre-image processing using Wallis Filter (Wallis, 1976) which is expressed as following equation.

$$g^c(x,y) = \left[g(x,y) - m_g\right]\left(c \cdot s_f\right)/\left(c \cdot s_g + s_f / c\right) + b \cdot m_f + (1-b)m_g \quad (10)$$

where, $g^c(x,y)$: Enhanced image function of the window, $g(x,y)$: Image function of the window, m_g: Mean gray level for window of original image, s_g: Standard deviation for window of original image, m_f: Target value for window of original image, s_f: Target value for Standard deviation of original image, c: Contrast ratio, b:Threshold for gray level.

Figure 9 shows enhanced image by Wallis Filter using m_f=127, s_f=87, b=0.5, c=3.

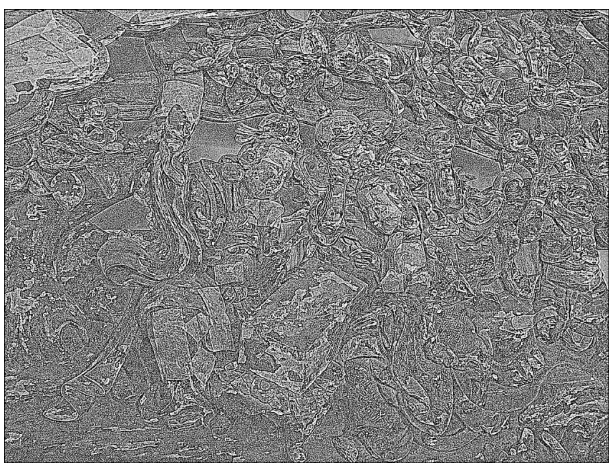

Figure 9. Enhanced image by Wallis Filter
(window size=7×7)

5.4 Extraction of feature point

There are many operators for extraction of feature point or detection of edge such as Canny (Canny, 1986), Harris (Harris, 1988) and Susan operator (Smith, 1995). However, Moravec operator (Moravec, 1981) was used for the enhanced image in this paper from the reasons that the relief was formed with curved surface and its processing ability. Equation (11) shows Moravec operator and Figure 10 shows extracted feature points by Moravec operator.

$$g(i,j)=\frac{1}{8}\sum_{k=i-1}^{i+1}\sum_{l=j-1}^{j+1}\left(g(k,l)-g(i,j)\right) \qquad (11)$$

where, g( ): Gray level

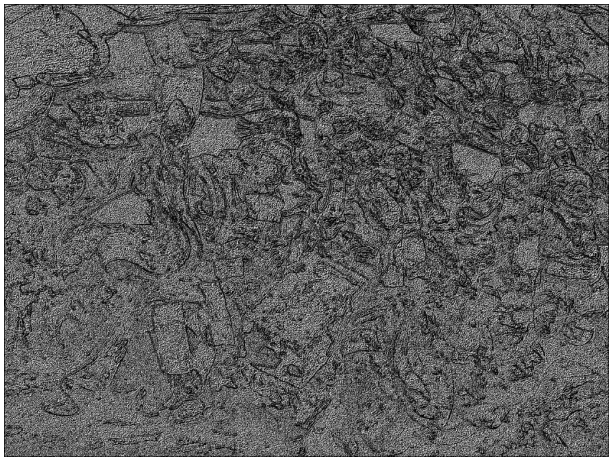

Figure 10. Extracted feature points by Moravec operator

5.5 3D Modelling

Generally, textured 3D models used to express using TIN model. In order to express 3D model for curved surface object, point cloud data were generated from stereo image matching using epipolar geometry and Least Square matching techniques (Gruen, 1985).

Figure 12(a) shows 3D point cloud model for the stereo pair which was taken by the IBIM system. In order to make reality, texture for each point was mapped using 3D coordinate for each point and calibration results. Figure 12 (b) shows textured 3D point cloud model.

It can be seen that the reality was improved but there are many occlusions which were caused by complex structure. In order to complement occlusions, additional stereo pairs which were taken upper and lower were applied. Figure 12 (c) shows 3D model which was generate using two stereo pairs (front pair and upper pair), Figure 12 (d) shows 3D model using 3 stereo models (upper, front, lower).

Obviously, It can be seen that occlusions are complemented according to additional stereo pairs. In particular, lower stereo pair was efficient to complement of occlusion parts.

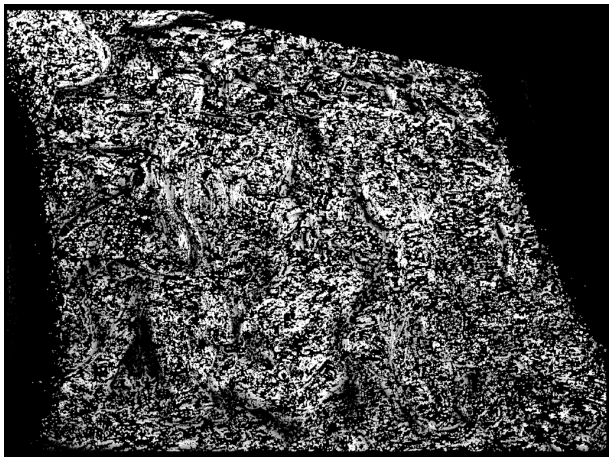

Figure 12(a). 3D point cloud model

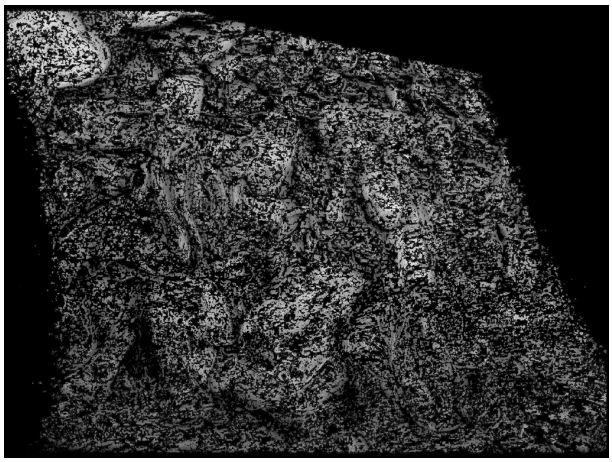

Figure 12(b). 3D point cloud model with texture

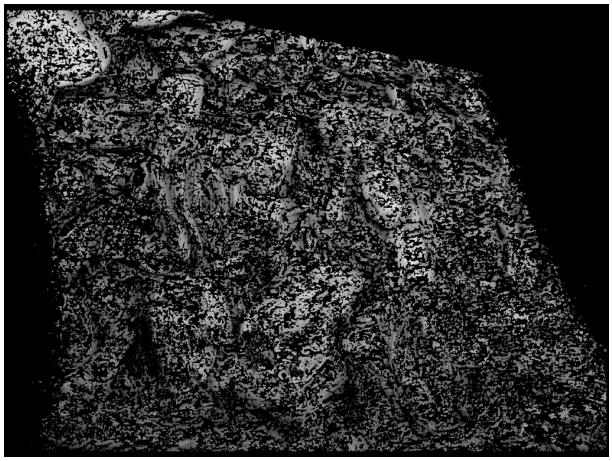

Figure 12(c). 3D point cloud date using 2 stereo pairs

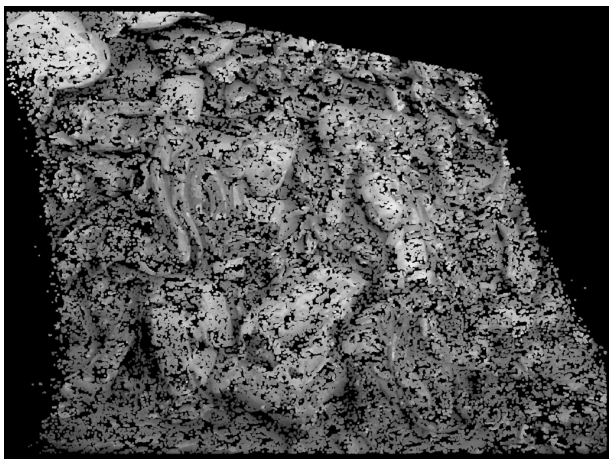

Figure 12(d). 3D point cloud date using 3 stereo pairs

6. CONCLUSIONS AND FURTHER WORKS

The Image Based Integrated Measurement (IBIM) System using digital camera and laser distance meter was developed by the authors for a convenient digital photogrammetry, and performance evaluation was investigated in this paper.

The new calibration method using distances between camera and temporal GCPs verified that the same accuracy is acquired compare with theoretical value. Moreover, the IBIM system established non-destruction measurement environments.

Furthermore, stereo matching for all pixels were investigated, and 3D model for complex structures such as curved surface were expressed as 3D point cloud model using additional stereo pairs.

Therefore, it is concluded that the IBIM is expected to become a useful measurement system for the various close range application fields since interior orientation parameters and exterior orientation parameters are calibrated simultaneously without any scale distances nor GCPs on object field.

There are issues, however, for further work. These problems are image matching procedures for 3D modelling and integration of 3D models.

References from Other Literature:

Canny, J. F., 1986, A computational approach to edge detection, IEEE Trans. Pattern Analysis and Machine Intelligence, 8: pp. 679-698

Chikatsu, H. and Kunii, Y., 2002, Performance Evaluation of Recent High Resolution Amateur Cameras and Application to Modeling of Historical Structure, International Archives of Photogrammetry and Remote Sensing, Vol.XXXIV, Part5, pp. 337-341, Corfu

Clive S. Fraser, 1996, Design Aspects of Utilizing Digital Photogrammetry for Deformation Measurements, Proceedings of the 8th FIG International Symposium on Deformation Measurements, pp.115-123, Hong Kong

Fryer, J. G. and Brown, D.C., 1986, Lens Distortion for Close-Range Photogrammetry, Photogrammetric Engineering and Remote Sensing, Vol.52, No.1, pp. 51-58.

Gruen, A., 1985, Adaptive least squares correlation: A powerful image matching technique, South Africa Journal of Photogrammetry, Remote Sensing and Cartography, Vol.14, No.3, pp.175-187

Harris, C. G., and Stephens, M., 1988, A combined corner and edge detector, 4th Alvey Vision Conference, pp.147-151

Kunii, Y., and Chikatsu, H., 2001, On the Application of 3 Million Consumer Pixel Camera to Digital Photogrammetry, Proceedings of SPIE (Videometrics VII), Vol.4309, pp. 278-287

Moravec, H., 1981, Rover visual obstacle avoidance, In International Joint Conference on Artificial Intelligence, Vancouver, British Columbia, pp. 785-790

Ohdake, T., and Chikatsu, 2004, H., Development of Image Based Integrated Measurement System and Performance Evaluation for Close-Range Photogrammetry, International Archives of Photogrammetry and Remote Sensing, Istanbul, Vol.XXXV, Com5, pp. 296-301

Smith, S. M., and Brady, J. M., 1995, SUSAN-a new approach to low level image processing, Defence Research Agency Technical Report, TR95SMSlb

Wallis, R., 1976, An approach to the space variant restoration and enhancement of images, Proc. of Symp. on Current Mathematical Problems in Image Science, Naval Postgraduate School, Monterey CA, USA, November, pp.329-340.